PRELIMINARY DESIGN OF A SOLAR POWERED TAILLESS MOTORGLIDER

Giorgio GUGLIERI[+]
Fulvia QUAGLIOTTI[*]

Politecnico di Torino
Dipartimento di Ingegneria Aeronautica e Spaziale
Corso Duca degli Abruzzi, 24 - 10129 Torino (Italy)

Abstract

In this paper, the requirements for the design of a solar powered tailless motorglider are discussed. An introductory comparison with conventional two surfaces aircraft demonstrates that the all wing configuration is competitive, even if some more typical aspects must be considered in detail. A feasibility study concerning this subject is presented, based on the parametric study of wing characteristics, in which aircraft aerodynamics and performances are directly evaluated for a complete set of possible configurations.
The conclusions demonstrate that the design of a tailless solar powered motorglider is feasible.

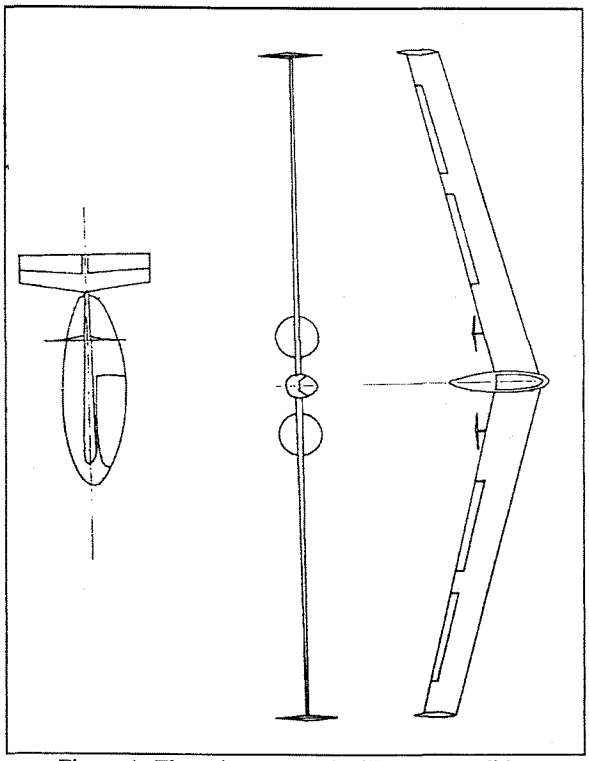

Figure 1: The solar powered tailless motorglider

Nomenclature

b	Wing span	(m)
c	Wing chord (b/λ)	(m)
c_a	Mean aerodynamic chord	(m)
c_e	Elevator (elevon) geometric chord	(m)
c_r	Wing root chord	(m)
c_t	Wing tip chord	(m)
C_D	Drag coefficient $\left(C_D = D/\left(\frac{1}{2}\rho V^2 S\right)\right)$	
C_L	Lift coefficient $\left(C_L = L/\left(\frac{1}{2}\rho V^2 S\right)\right)$	
$C_{L\alpha}$	Lift coefficient derivative (stick fixed)	
$C_{L\alpha}$*	Lift coefficient derivative (stick free)	
C_{Lq}	Longitudinal damping derivative	
$C_{L\delta}$	Control derivative $dC_L/d\delta$	
C_l	Rolling moment coefficient	
C_{lp}	Roll damping derivative	
$C_{l\delta}$	Control derivative $dC_l/d\delta_a$	
C_m	Pitching moment	
C_{mq}	Longitudinal damping derivative	
C_{mO}	Pitching moment (C_L=0)	
$C_{mO\delta}$	Control derivative $dC_{MO}/d\delta$	
D	Aerodynamic drag force	(N)
d_m	Distance between propeller axis and longitudinal x axis	(m)
E	Aerodynamic efficiency $(L/D = C_L/C_D)$	
E_A	Available energy for climbing flight	(J)
E_N	Required energy for climbing flight	(J)
G	Stick gain	(rad/m)
g	Gravitational acceleration	(m/s^2)
H	Hinge moment	(Nm)
I	Solar irradiation	(W/m^2)
Kn	Stick fixed static margin	
Kn'	Stick free static margin	
Km	Stick fixed maneuver margin	
Km'	Stick free maneuver margin	
L	Aerodynamic lift force	(N)
n	Load factor	
N_δ	Yawing moment control derivative	(Nm)
N_β	Yawing moment derivative	(Nm)
P	Stick force	(N)
P_A	Available power for level flight	(W)

[+] Assistant Professor, member AIAA-AHS
[*] Associate Professor, member AIAA

P_N	Required power for level flight	(W)
r	Taper ratio (c_t/c_r)	
Re	Reynolds number ($\rho Vc/\mu$)	
S	Wing surface	(m^2)
S_C	Surface covered by solar cells	(m^2)
S_e	Elevator (elevon) reference surface	(m^2)
T	Propeller thrust	(N)
t	Time	(s or h)
V	Flight airspeed	(m/s)
x_G	Coordinate of center of gravity	(m)
x_M	Coordinate of stick fixed maneuver point	(m)
x_M*	Coordinate of stick free maneuver point	(m)
x_N	Coordinate of stick fixed neutral point	(m)
x_N*	Coordinate of stick free neutral point	(m)
Y_δ	Side force control derivative	(N)
Y_β	Side force derivative	(N)
w	Vertical speed	(m/s)
W	Aircraft weight	(N)
W_B	Weight of batteries	(N)
α	Angle of attack	(deg)
δ	Elevator (elevon) deflection	(deg)
δ_a	Aileron deflection (elevon)	(deg)
δ_r	Rudder deflection (elevon)	(deg)
γ	Climb angle	(deg)
Γ	Dihedral angle	(deg)
ε	Wing tip twist angle	(deg)
ϕ	Bank angle	(deg)
η	Global efficiency	
ηp	Propeller efficiency	
λ	Aspect ratio (b^2/S)	
Λ	Sweep back angle	(deg)
μ	$2m/\rho Sc_a$	
μ	Air viscosity	(Kg/m/s)
ρ	Air density	(Kg/m^3)
σ	Surface ratio(S_C/S)	
ξ	Battery energy rate	(Wh/Kg)

Subscripts

CF	Climbing flight condition
FUS	Fuselage
LF	Level flight condition
VT	Vertical tail
max	Maximum
min	Minimum

Introduction

A solar powered flying machine is an extremely attractive challenge for any aircraft designer. Many attempts were made in the past and some of them were very successful [1].

Several limitations - due to the low efficiency of the energy conversion process - concentrate the attention on very light aircraft, such as motorgliders, designed for low speed flight.

The configurations adopted are generally based on the coupling of two lifting surfaces (e.g. Solair I, Solar Challenger, Sunseeker), both of them covered by solar cells.

This design is selected as a consequence of some advantages. The wing is moderately swept, so that the manufacturing is simplified. As the spanwise lift distribution is very close to the elliptic shape, the induced wing drag is minimized. The longitudinal control is obtained with conventional movable surfaces, and the stability margin can be easily modified, after preliminary tests, by changing either the incidence or the location of wing and tailplane (or canard), without any significant configuration change. Furthermore, a moderate excursion of center of gravity is possible, without compromising stability.

These relevant arguments can explain the choice of a conventional configuration for a solar powered motorglider, when the primary goal for the designer is making it fly.

Differently, when the primary aim is the optimization of the performances (i.e. endurance), the selection of different configurations may be considered and a possible competitive candidate could be the flying wing [2].

The primary advantage of this choice is the minimization of parasite drag for tailless aircraft, with the dual impact of increasing aerodynamic efficiency and reducing power requirements for best endurance.

Most of wing surface can be easily covered by solar cells and the particular spanwise aerodynamic loading minimizes structural stress and cell damage (the compliance of solar cells is usually limited), reducing the aircraft structural weight fraction. Hence, larger aspect ratios and wing spans are acceptable, with respect to conventional unswept wings.

Nevertheless, some important disadvantages of tailless aircraft must be discussed [3].

The first problem is the possibility of autorotation in pitch (i.e. tumbling), due to a rapid nose pitch-up at low speed. This behaviour is typical of statically unstable configurations (mainly at high angle of attack). Autorotation is usually avoided when the static margin is positive. An increase of sweep angle is generally beneficial too.

The second problem is the lack of pitch and yaw damping: some pilots made negative comments about handling qualities of tailless solutions, due to the tendency to pilot induced oscillations (PIO) under adverse flight conditions (rough air). This dangerous tendency can be generally eliminated by increasing wing sweep angle Λ.

Another serious problem involves the aerolastic behaviour. Increasing the wing sweep in order to improve handling qualities and to reduce the possibility of tumbling, the aerolastic coupling between wing flap bending and pitch motion is promoted, resulting in limited pitch stability at

high speed. The way to alleviate this problem is the correct dynamic balancing of elevons.
Furthermore, the stability requirements are generally satisfied by the designer with an appropriate selection of wing sweep and twist. Unfortunately, the resulting spanwise lift distribution is far from being elliptic. As a consequence, the higher induced drag penalizes this wing geometry, when compared with conventional unswept lifting surfaces. Anyway, larger aspect ratios (possible with tailless aircraft) minimize the disadvantage.
Finally, the maximun lift coefficient is reduced by increasing Λ (stall speed is increased). Moreover, the sweep back deflects the surface flow and the boundary layer towards the wing tip, affecting stall and stability characteristics around the yaw axis during flight with sideslip [4,5].
The aforementioned disadvantages of the tailless design can be eliminated or minimized by means of a detailed preliminary design procedure. A simplified* feasibility analysis concerning this subject is given hereafter, where the primary aim is to demonstrate that the design of a tailless solar powered motorglider is possible and the additional complexity introduced is acceptable.
The analysis is based on a parametric study of wing characteristics, in which aircraft aerodynamics and general performances are directly evaluated for a complete set of possible configurations.

Aerodynamics

The performance evaluation of a tailless solar powered aircraft is strictly coupled with the aerodynamics of flying wings.
Two significant questions concern the activity of the aerodynamicist:
1) the choice of the wing airfoil,
2) the evalutation of the wing characteristics for a given configuration (λ, Λ, ε, r).
The selection of a wing airfoil should be the result of a compromise between required aerodynamic characteristics (i.e. E_{max} , C_{Lmax}) and operative prerequisites.
Several high lift airfoils were designed [6,7] for the limited speed range ($Re=10^6$), where the solar powered motorgliders can normally fly, due to their limited power-to- weight ratios P_A/W. Anyway, these highly cambered airfoils cannot be adopted for the application under consideration: generally solar cells must be fixed on an almost flat surface, in order to obtain a uniform solar irradiation and a higher panel stiffness.
As a consequence, a lower performance airfoil with flat upper surface was chosen: the Lissaman-Hibbs 8025 [8]. This airfoil was used by MacCready in the design of Solar Challenger. The results of the flight tests were satisfactory, although wind tunnel data were not available. Only recently test have been performed, and the aerodynamic coefficients for this wing section were obtained in the D3M low speed wind tunnel at Politecnico di Torino. The static force and pressure measurements were performed for Re= 360000÷1560000 and V = 10÷50 m/s on an unswept wing with endplates (c = 0.5 m , b = 2 m and $\lambda = 4$).
Static forces were measured with an external six components balance and the model with endplates was supported by a vertical strut.
Static longitudinal data and angles of attack were corrected for buoyancy, solid and wake blockage effects.
Profile aerodynamic coefficients were derived by means of an extension of the analytical method developed in Refs [9,10]. This procedure is based on the comparison of longitudinal coefficients for the wing model both with and without endplates.
Finally the effective equivalent aspect ratios of the model panel with endplates were extimated: $\lambda_\sigma = 5.99$ and $\lambda_\tau = 5.34$ where $\alpha_i = C_L/\pi\lambda_\tau$ and $C_{Di} = C_L^2/\pi\lambda_\sigma$.
This correction was adopted in order to compute the effective profile drag and angles of attack.
Pressure ports were distributed chordwise (32 ports) at 50% of the left wing semispan. Spanwise measurements were also performed (8 ports) at maximum profile thickness on the leeward side of the model.
The results demonstrate that stagnation point ($c_p = 1$) is located on the leading edge for very low angles of attack, while for higher incidence this point shifts in the ventral part of the profile.
The presence of a laminar separation bubble with flow reattachment on the leeward side of the wing is also evident. The extension of separation is reduced at higher Reynolds numbers. Furthermore, flow separation at stall is propagated abruptly.
A satisfactory comparison between balance and pressure measurements of C_L amd C_m coefficients was also performed.

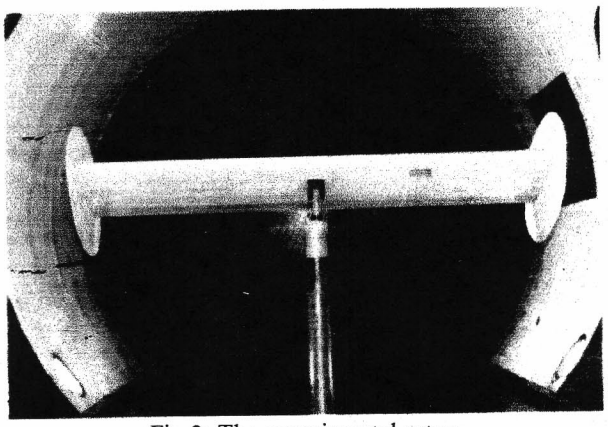

Fig.2: The experimental setup

*Some restrictions apply to the present analysis:
1) low altitude flight is assumed
2) control surfaces are supposed to be effective in the airspeed range considered.

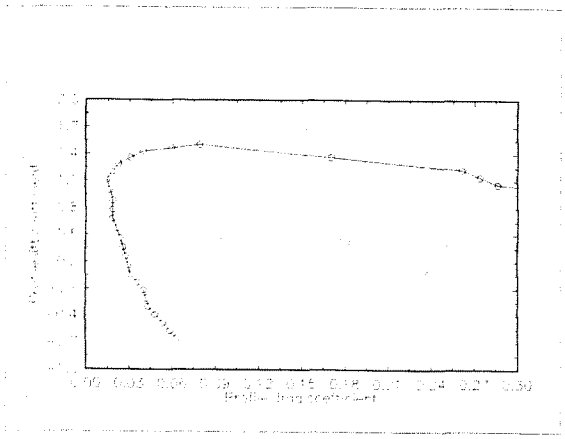

Fig. 3: The profile lift and drag coefficients (Re=970000)

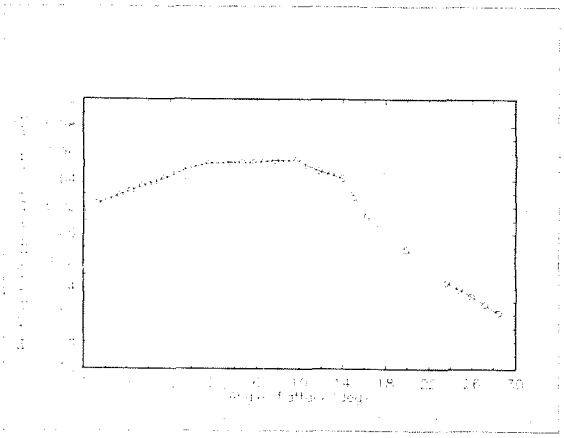

Fig.4:The profile pitching moment coefficient (Re=970000)

Some general conclusions concerning these experimental results can be summarized:

1) the behaviour is critical for lower Reynolds number,

2) the drag decreases moderately with angle of attack, having a minimum for positive α,

3) the pitching moment coefficient is moderately positive (i.e. stable) for incidence below stall

4) E_{max} and $\left(E\sqrt{C_L}\right)_{max}$ occur at the same angle of attack,

5) the separated flow at wing stall propagates abruptly along the lifting surface.

The evaluation of wing characteristics as a function of design parameters is performed by means of Weissinger method [11,12] - an extension of lifting line theory - which permits to evaluate the effects of sweep in incompressible flow with accetable reliability, when a comparision is made with other advanced computational methods, which are generally time consuming. On the contrary, this simplified theory is able to analyse a wide number of configurations using a standard PC, requiring a minimum computational time.

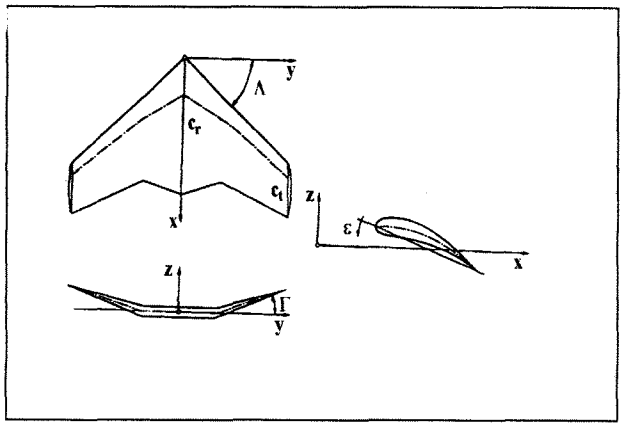

Figure5 :The flying wing configuration

Performances

The configuration selected is a flying wing, with a profiled ogival fuselage along the root chord, where the pilot is seated in an inclined position (see Fig.1).

The aircraft longitudinal and lateral controls are performed by means of differential deflections of elevons, while directional control is obtained using conventional rudders, hinged on vertical wing tip fins [13]. It has to be noted that, wing tip section must be able to withstand loads induced by both vertical stabilizer and ground handling (highly tapered wings are critical).

Spoilers should be provided for speed control during glide or dive.

The landing gear is profiled in order to minimize drag in cruise flight. Shock absorbing devices are for minimizing cells damage during take off and landing.

The solar cells are fixed on the wing upper surface and electrically connected, so that series of panels are obtained (photovoltaic generator). The electrical power supplies a motor, which drives a reduction gearbox and a propeller.

The thrust axis is supposed aligned with the wing root chord, i.e. no pitching moment is generated by thrust. Therefore, the static longitudinal stability of the wing is mainly influenced by the neutral point and center of gravity locations.

The thrust is generated by a propeller, designed for high efficiency at low speeds in different flight conditions, that means large propeller diameter and low rotation rates, with controllable blade angle. This propeller should reach good efficiences (ηp = 0.9 in level flight), even if several geometrical interference problems are introduced in the design (i.e. ground clearence during take off and landing). As a consequence, the possibility of adopting two separate smaller propellers must be considered.

Moreover, the available energy for take off and climbling from ground to flight altitude (generally lower than 1000 m) obtained by the photovoltaic conversion process is limited. Hence, a second spare voltage supply unit (accumulators) is required, recharged by solar cells during

ground stops. A relevant weight fraction is introduced due to the presence onboard of batteries.
As a conclusion, two typical flight conditions should be analysed:
1) solar powered lever flight,
2) battery powered climbling flight.
The selection of accetable performances and safety conditions determine the severe constraints in the definition of wing design characteristics.

Level flight conditions

The primary question is the comparison of required power and energy with those ones available from direct solar radiation. This last term is generally small and seriously affected by external factors such as adverse weather, pollution, cell orientation, latitude and local time.
All preliminary calculations are performed considering a conventional reference mean solar irradiation (I = 500 W/m^2).
The energy conversion process (substantially influenced by photovoltaic and mechanical effects) reduces dramatically the available power for aircraft propulsion.
Hence, global efficiency (obtained by multiplying motor, gearbox, propeller and photovoltaic efficiencies) is limited to $\eta = 0.10 \div 0.15$.
We obtain that:

$$P_A = \eta \sigma S I$$

The required power is related with the equilibrium of the external loads acting on the aircraft during level flight.
Hence:

$$P_N = TV_{LF} = DV_{LF}$$

By combining the formulation of aerodynamic efficiency E with the formulation of cruise airspeed $V_{LF} = \sqrt{2W/\rho S C_L}$
We find that

$$P_N = \frac{V_{LF} W}{E} = \sqrt{\frac{2}{\rho}} \frac{1}{E\sqrt{C_L}} \sqrt{\frac{W}{S}} W$$

Climbing flight conditions

The analysis of climbing flight is performed taking into account the effects of battery powered propulsion only.
The characteristics of batteries are expressed in terms of costant energy output related with a time interval, and usually this energy output decreases as required power increases (or alternatively output time interval decreases).
Several types of accumulators are available but their performances are substantially different. In the present discussion, Ni-Zn batteries are used for the propulsion of the motorglider, and therefore the energy output is $\xi \leq 60 Wh/Kg$ as a function of specific power: $\xi = f(P_{CF}, W_B)$.
The choice of a different type of accumulator is possible (note that climbing time t_{CF} is generally much lower than 1h), but lower performances introduce higher battery weight fractions (lead-acid batteries) and low discharge efficiencies ξ/ξ_O, while higher performances batteries are not compatible with low energy-to-power rates (i.e. low discharge time intervals), required for reaching the cruise altitude in few minutes.
Within these assumptions, it is possible to evaluate the available energy for climbing flight, using the following simple equation:

$$E_A = \xi \frac{W_B}{g}$$

The energy required for climbing flight from ground to a selected altitude (we consider flight at 500 m with constant vertical speed w = 2.5 m/s and t_{CF} = 200 s) is obtained through the equilibrium of forces acting on the aircraft in these conditions:

$$\begin{cases} L = W\cos\gamma \\ T = D + W\sin\gamma \end{cases}$$

Introducing the aerodynamic efficiency E in the second of these two equations and multiplying by V_{CF}, we find that

$$P_N = \frac{W\cos\gamma}{E} V_{CF} + W V_{CF} \sin\gamma$$

where $w = V_{CF}\sin\gamma$, and

$$P_N = \frac{W\cos\gamma}{E} V_{CF} + Ww$$

If we consider that usually $\gamma \approx 0$, it is possible to derive that $\cos\gamma \approx 1$ and $L \approx W$. We obtain:

$$P_N \approx \frac{V_{CF} W}{E} + Ww = DV_{CF} + Ww$$

Finally, the formulation of required energy is obtained:

$$E_N = \frac{P_N t_{CF}}{\eta_P}$$

where η_p is the propeller efficiency during climb ($\eta_p \approx 0.6$ in climb conditions).

Aircraft weight fractions

The weight of the aircraft is a linear function of a wing surface S:

$$W = W_0 + k_1 g S + k_2 g \sigma S + W_B$$

where k_1 is the surface density of a wing built in composite material (k_1 = 2.5 Kg/m^2) and k_2 = 1 Kg/m^2 is the solar cell surface density (Silicium type).
The surface ratio σ is fixed at 80%.
The term W_0 = 1420 N is the addition of several constant components:

- Pilot: 900 N
- Fuselage : 200 N
- Motor : 200 N
- Gearbox : 40 N
- Propeller : 80 N

The linear equation $W = f(S, W_B)$ is then directly related with P_A and E_A, as S and W_B increase with the power required for level flight and the energy necessary for climb respectively.

Parametric analysis

The comparison of available power versus required power and energy in the flight conditions considered, combined with the weight fractions equation, defines S and W_B. Consequently, the solar powered level flight and the battery powered climb are possible for the specified conditions, where a 20% margin is introduced. Remind that, an important limiting factor is induced by cell heating that can reduce solar cell efficiency (0.5 % / °C decrement). Even winds or gusts can affect aircraft power requirements.

We obtain:

$$\begin{cases} P_A = 1.2P_N \ \text{(level flight)} \\ E_A = 1.2E_N \ \text{(climb)} \end{cases}$$

As $\gamma \approx 0$, we obtain that

$$V = V_{LF} \approx V_{CF}$$

In order to solve this system of equations, the airspeed V corresponding to cruise and climbing flights must be specified. This means that the aircraft should fly at a selected angle of attack, with related lift coefficient C_L, aerodynamic efficiency E and optimal factor $E\sqrt{C_L}$, which define together a unique possible airspeed for a given altitude.

Generally, the two angles of attack (or C_L) at which a conventional aircraft with propellers reaches optimal level and climbing flight conditions are substantially different, and usually minimum energy climb attitude (i.e. maximum $E\sqrt{C_L}$) is found at dangerously high α, that means very low speed in the vicinity of wing stall (unsafe flight).

Due to the particular aerodynamic behaviour of the profile adopted for this solar powered tailless motorglider (LH 8025), the two conditions are almost cohincident with stall angle of attack (minimum power level flight and minimum energy for climb occur almost at the same α at $C_L \approx C_{L,max}$).

With the aim of ensuring a safe flight, optimal flight attitude cannot be adopted, and a 20% increase in airspeed V (i.e. 70 % lift coefficient reduction) is necessary:

$$\begin{cases} V = 1.2V_{min} = 1.2\sqrt{\dfrac{2W}{\rho S C_{L,max}}} = \sqrt{\dfrac{2W}{\rho S C_L}} \\ C_L = 0.7C_{L,max} \end{cases}$$

Using the Weissinger theory it is possible to evaluate the magnitude of C_L and $E\sqrt{C_L}$ as a function of aspect ratio λ and sweep angle Λ, for given taper ratio (r = 0.7) and twist angle ($\varepsilon = 3°$).

Therefore, for any given $E\sqrt{C_L}$ (i.e. λ, Λ), the variables S and W_B are obtained with the iteration of the following equations:

$$\begin{cases} \eta\sigma IS = 1.2\sqrt{\dfrac{2}{\rho}}\dfrac{1}{E\sqrt{C_L}}\sqrt{\dfrac{W}{S}}W \\ \xi\dfrac{W_B}{g} = \dfrac{1.2t_{CF}}{0.99\eta_p}\left\{\sqrt{\dfrac{2}{\rho}}\dfrac{1}{E\sqrt{C_L}}\sqrt{\dfrac{W}{S}}W + Ww\right\} \end{cases}$$

where a 1% increment is introduced in the second equation taking into account drag and friction during take off run.

By means of the two terms S and W_B, the aircraft weight W, the mean chord c, the span b, the power P_A and the energy E_A are easily derived.

The complete wing geometry is finally defined, as a function of aspect ratio λ and sweep angle Λ. Note that the effect of global efficiency η on the solutions is not marginal.

These solutions are obtained with the above described deterministic procedure, and a unique wing geometry is found for each given $E\sqrt{C_L}$ or (λ, Λ).

All these configurations are compatible with the requirements of P_A for level flight and E_A for climb. Anyway, only a limited subset has a practical interest for the designer.

As an example, when the aspect ratio λ is too small, the wing surface S and the weight W become too large and unacceptable, due to the typical induced drag penalty (i.e. an excessive increase of P_N and E_N), although the aircraft configuration respects the energy requirements for flight.

On the contrary, the benefits on performances for very high aspect ratio wings are negligible, even if the manufacturing and the structural design become extremely complex. Furthermore, the reduction of chord lenght c and local Reynolds number, particularly in the vicinity of the tips, may change abruptly wing stall characteristics and lateral control effectiveness. Finally, the wing loading W/S could increase too much and the power-to-weight ratio P_A/W could become too low.

Hence, in order to distinguish the acceptable configurations, some selection criteria must be adopted for the analysis of the results:

- a) $W \le W_{max}$ (e.g. $W_{max} = 3000N$)
- b) $Re \ge Re_{min}$ (e.g. $Re_{min} = 775000$ for LH8025)
- c) the minimum sink rate w in power off flight must be limited
- d) the maximum efficiency $E \ge E_{min}$ (e.g. $E_{min} = 20$)
- e) the stall airspeed V_{min} must be minimized
- f) the span b must be limited for wing transport
- g) $\lambda \ge \lambda_{min}$ (e.g. $\lambda_{min} = 5$)

Some of these constraints are generally more effective in selecting the set of acceptable solutions: for the initial conditions considered, the limitations on weight and Reynolds number exclude the lower and the higher aspect ratio wings respectively, while the other controls are almost uneffective.

A final selection is required in order to discard statically unstable flying wings. The criterium for stability is a positive static margin, i.e. the center of gravity must be located forward of the neutral point. This last control typically eliminates low sweep angle wings, as the increase of Λ has a stabilising effect, due to the rearward shift of neutral point. Note that tailless aircraft are extremely sensitive to the shift of the center of gravity location, due

to the uncommon concentration of mass in the vicinity of pitch axis.

The final set of acceptable solutions is given in Fig. 9 , in which the characteristics of several all wing aircraft (gliders and motorgliders) are compared. The wing loading of these reference aircraft ranges from 64 N/m^2 to 375 N/m^2 (se also Refs. [14,15]).

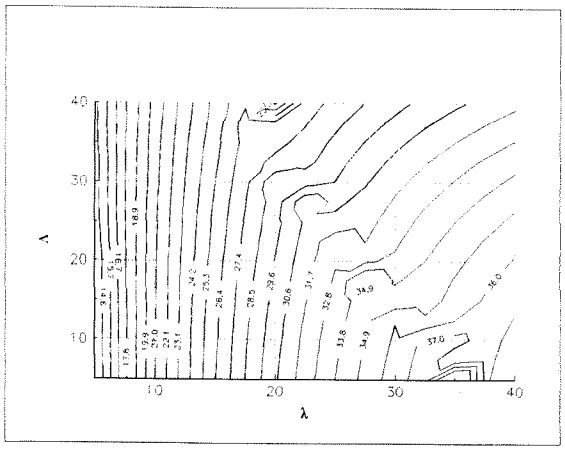

Figure 6: The parameter $E\sqrt{C_L}$ as a function of aspect ratio λ and sweep angle Λ

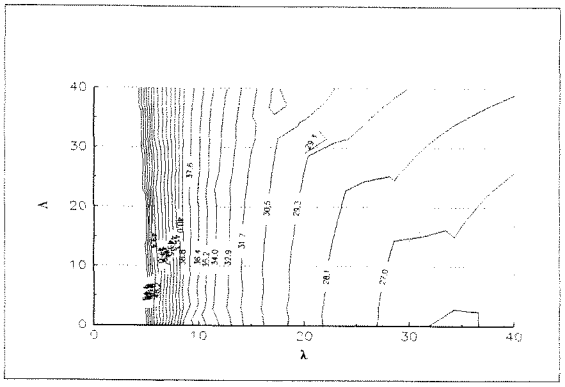

Figure 7: The wing surface S as a function of λ and Λ for η = 0.125

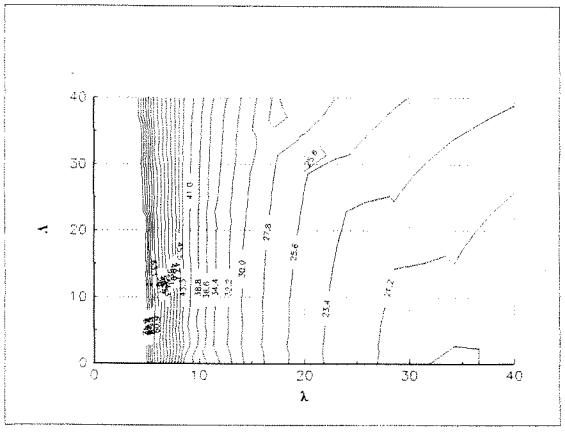

Figure 8: The weight of batteries W_B as function of λ and Λ for η = 0.125

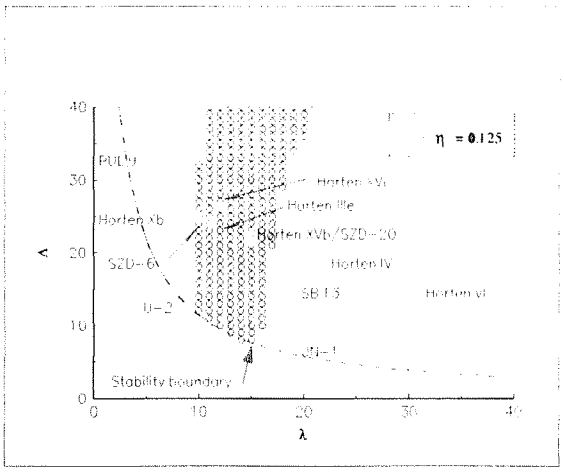

Figure 9: Comparison of compatible solutions for η=0.125 with several conventional all wing gliders and motorgliders.

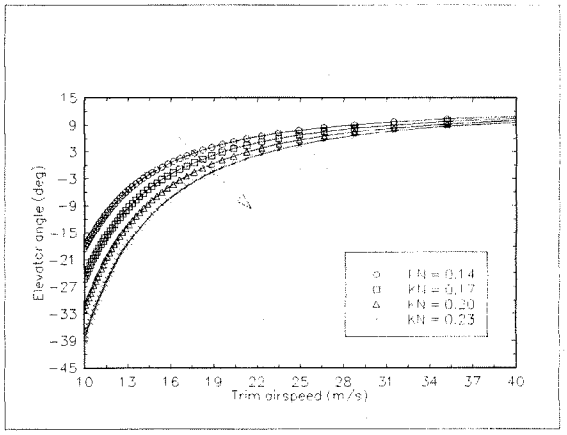

Figure 10: The effect of static margin **Kn** on elevator deflection.

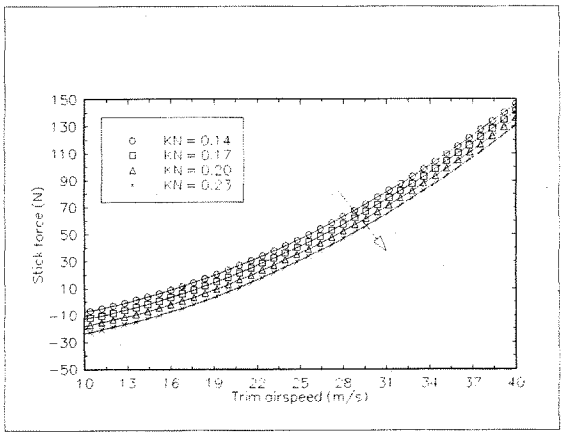

Figure 11: The effect of static margin **Kn** on stick force.

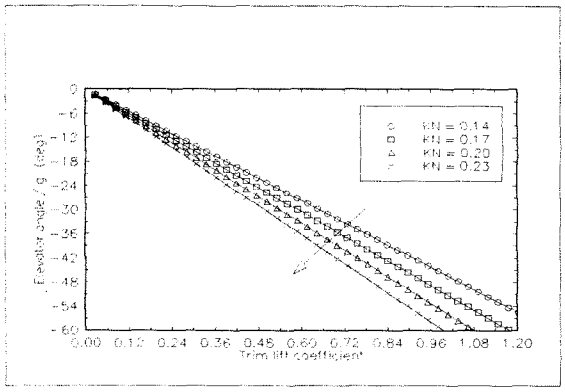

Figure 12: The effect of static margin **Kn** on elevator gradient **dδ/dn**.

$\Lambda = 15°$	$W = 2700$ N
$\lambda = 13$	$W/S = 85.26$ N/m^2
$b = 20.29$ m	$W_B = 320$ N
$c = 1.561$ m	$C_{L,max} = 1.343$
$c_a = 1.577$ m	$(E\sqrt{C_L})_{max} = 24.1$
$S = 31.67$ m^2	$V_{min} = 10.2$ m/s

Tab. 1: The reference configuration.

Kn	C_{Lq}	C_{mq}
0.140	3.588	-2.873
0.170	3.864	-3.020
0.200	4.140	-3.184
0.230	4.416	-3.363

Tab. 2: The effect of static margin **Kn** on longitudinal damping derivatives.

Configuration analysis

Among the acceptable configurations an example was selected in order to evaluate the general aeromechanical characteristics of this solar powered tailless motorglider (see Tab. 1).
General aerodynamics, static derivatives and control effectiveness were computed. Longitudinal damping and hinge derivatives were estimated (Refs [16,17]).

Kn	**Kn'**	**Km**	**Km'**	**dP/dn** (N)
0.140	0.099	0.371	0.330	-45.8
0.170	0.129	0.419	0.378	-51.2
0.200	0.159	0.468	0.427	-56.6
0.230	0.189	0.520	0.479	-62.0

Tab. 3: Stick fixed/free static margins - stick fixed/free maneuver margins - stick force gradient dP/dn

The static stability of this wing geometry was also verified:

$$Kn = -\frac{(x_G - x_N)}{c_a} = 0.22 .$$

Elevator deflections, stick forces, steady pull-up gradients and stability margins were derived at sea level for several center of gravity locations x_G.
The following equations apply:

$$\begin{cases} \delta_{EQ} = \dfrac{C_{L\alpha}}{\Delta}\cdot\left(C_{mO} - Kn\cdot\dfrac{2W/S}{\rho_O}\cdot\dfrac{1}{V_{EQ}^2}\right) \\ \Delta = C_{L\alpha}\cdot C_{mO_\delta} \end{cases}$$

$$\begin{cases} P = P_O + B\cdot\dfrac{1}{2}\rho_O V^2 \\ P_O = -G\cdot S_e c_e\cdot W/S\cdot\dfrac{C^*_{L\alpha} b_2}{\Delta}\cdot Kn' \\ B = -G\cdot S_e c_e\cdot\left(C_{mO}\dfrac{b_1 C_{L\delta} - b_2 C_{L\alpha}}{\Delta}\right) \\ H = \dfrac{1}{2}\rho_O V^2\cdot S_e c_e\cdot(b_O + b_1\alpha + b_2\delta) \\ C^*_{L\alpha} = C_{L\alpha}\cdot\left(1 - \dfrac{b_1 C_{L\delta}}{b_2 C_{L\alpha}}\right) \\ Kn' = -\dfrac{(x_G - x^*_N)}{c_a} \end{cases}$$

$$\begin{cases} \dfrac{d\delta}{dn} = -\dfrac{C_{L\alpha}}{\Delta}\cdot(C_L)_{n=1}\cdot\left(1 - \dfrac{C_{Lq}}{2\mu}\right)\cdot Km \\ Km = -\dfrac{(x_G - x_M)}{c_a} \end{cases}$$

$$\begin{cases} \dfrac{dP}{dn} = -G\cdot S_e c_e\cdot W/S\cdot\dfrac{C_{L\alpha}}{\Delta}\cdot\left(1 - \dfrac{C_{Lq}}{2\mu}\right)\cdot Km' \\ Km' = -\dfrac{(x_G - x^*_M)}{c_a} \end{cases}$$

The results (see Figs. 10,11,12 and Tab. 3) confirm that the achievement of acceptable aeromechanical characteristics is possible.
Lateral control requirements were tested (Ref [18]): using an appropriate combination of controls, it must be possible to reverse the direction of a turn with a 45° bank in one direction to a turn with a 45° bank in the opposite direction within t = b/3 seconds, when the turns are made at a speed of 1.4 V_{min}.
Hence:

$$\frac{\Delta\phi}{\delta_a} = -\frac{C_{l\delta}}{C_{lp}}\cdot\left\{t + \frac{J_X}{C_{lp}}\cdot\left(1 - e^{\frac{C_{lp}\cdot t}{J_X}}\right)\right\}$$

where $\Delta\phi = 90°$ and $t = b/3 = 6.76$ s. Elevons were supposed to extend from $y/(b/2) = 0.4$ to $y/(b/2) = 0.9$ with a flap chord ratio $c_e/c = 0.2$. The critical aileron deflection is $\delta_a = 22°$.
A configuration with two separate propellers is considered for directional control analysis with asymmetric thrust (T = 250 N) due to engine failure. The rudder deflection is computed for $V = 1.4\ V_{min}$ assuming that $S_{VT} = 3$ m^2.
The equations for directional trim are:

$$\begin{cases} \pm T \cdot d_m + N_{\beta FUS} \cdot \beta + N_{\beta VT} \cdot \beta + N_{\delta r} \cdot \delta_r = 0 \\ Y_{\beta FUS} \cdot \beta + Y_{\beta VT} \cdot \beta + Y_{\delta r} \cdot \delta_r = 0 \end{cases}$$

and

$$\delta_r = \pm T \cdot d_m \cdot \left[\frac{\left(\frac{Y_{\beta FUS} + Y_{\beta VT}}{Y_{\delta r} \cdot \left(N_{\beta FUS} + N_{\beta VT} \right)} \right)}{\left(1 - \frac{N_{\delta r} \cdot \left(Y_{\beta FUS} + Y_{\beta VT} \right)}{Y_{\delta r} \cdot \left(N_{\beta FUS} + N_{\beta VT} \right)} \right)} \right] = \pm 25°$$

Finally, loads due to acceleration and gusts were also verified (see Fig. 13).

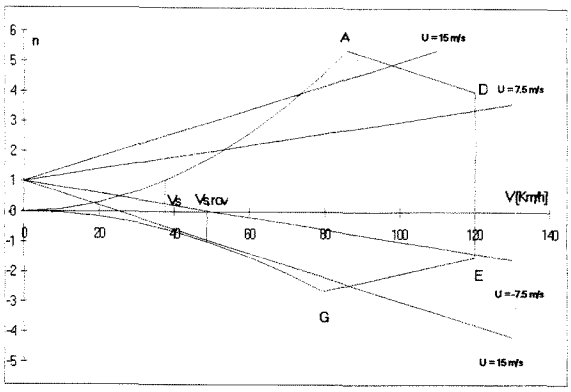

Fig.13 : The V-n diagram

Conclusions

The design of solar powered flying machines is limited to low speed light motorgliders, due to the penalized efficiency of the photovoltaic conversion process, even though many practical applications could be considered if more reliable sun powered aircraft were available.
Anyway a significant progress in this field will be possible only with advances both in solar energy conversion technology and specific aeronautical applied research.
With the aim of giving a contribution concerning this last subject, the present paper deals with the proposal for a tailless motorglider. The feasibility of a tailless aircraft design is discussed and confirmed by means of a simplified analysis of flight performances and aerodynamics, which could be easily extended, even for conventional configurations.

Acknowledgments

This research activity was carried out for the preliminary design of the Heliantus solar powered motorglider. Therefore, the authors would like to acknowledge Mr. P.L. Duranti and Mr. M. Borsi for their contribution and extraordinary support. A special thanks also for the students involved in this part of the program (Mr. S. Protto, Mr. V. De Maria and specially Mr. L. D'Angelo).

References

[1] MacCready, P.B., Lissaman, P.B.S., Morgan, W.R., Burke, J.D., *SunPowered Aircraft Designs*, J.of Aircraft, vol.20, n.6, June 1993.
[2] Nickel, K., Wohlfahrt, M., Tailless Aircraft in Theory and Practice, Edward Arnold, 1994.
[3] Culver, I.,*Tailless Flying Wings*, Technical Soaring, vol.XI, 1987.
[4] Horten, R., *Lift Distribution of Flying Wing Aircraft*, Technical Soaring, vol.X, 1986.
[5] Horten, R., *Flying Wing Geometry*, Technical Soaring, vol.XIV, 1990.
[6] Wortmann, F.X., *The Quest for High Lift*, AIAA 2nd Symp. on the Technology and Science of Low Speed and Motorless Flight, Cambridge, USA, 1974.
[7] Liebeck, R.H., *A class of Airfoils Designed for High Lift in Incompressible Flow*, J. of Aircraft, vol.10, n.10, October 1973.
[8] Lissaman, P.B.S., *Low Reynolds Number Airfoils*, Ann. Rev. Fluid. Mech., n.15, 1983.
[9] Rebuffet P., *Aérodinamique Experimentale*, 1962.
[10] Carafoli, *Aérodinamique des ailes d'avion*, Paris, 1928.
[11] Weissinger, J., *The Lift Distribution of Swept Back Wings*, NACA TM n.1120, 1947.
[12] De Young, J., Harper, C.H., *Theoretical Symmetric Span Loading at Subsonic Speeds for Wings having Arbitrary Plan Form*, NACA Rep. n. 921, 1948.
[13] Garbell, M.A., *Theoretical Principles of Wing Tip Fins for Tailless Airplanes and their Practical Application* , J. of Aeronautical Sciences, October 1946.
[14] Zientek, A., *Polish Flying Experience with Tailless Gliders*, Technical Soaring, vol. XVI, 1992.
[15] Gyorgyealvy, D., *Performance Analysis of the Horten IV Flying Wing*, 8th OSTIV Congress, Cologne, Germany, June 1960.
[16] Datcom USAF, *Stability and Control*, 1963.
[17] Etkin, B., *Dynamics of Flight - Stability and Control*, Wiley, 1982.
[18] OSTIV, *Airworthiness Requirements for Sailplanes*, 1976.